HHS Public Access

Author manuscript

Proc SPIE Int Soc Opt Eng. Author manuscript; available in PMC 2021 June 23.

Published in final edited form as:

Proc SPIE Int Soc Opt Eng. 2019 February ; 10871: . doi:10.1117/12.2510632.

An adaptive-coherence light source for hyperspectral, topographic, and flow-contrast imaging

Taylor L. Bobrow[a], **Nicholas J. Durr**[a]

[a]Department of Biomedical Engineering, Johns Hopkins University, 3400 N. Charles St., Baltimore, MD 21218. USA

Abstract

Colorectal cancer accounts for an estimated 8% of cancer deaths in the United States with a five-year survival rate of 55-75%. The early detection and removal of precancerous lesions is critical for reducing mortality, but subtle neoplastic growths, such as non-polypoid lesions, often go undetected during routine colonoscopy. Current approaches to flat or depressed lesion detection are ineffective due to the poor contrast of subtle features in white light endoscopy. Towards improving colorectal lesion contrast, we present an endoscopic light source with custom laser channels for multimodal color, topographic, and speckle contrast flow imaging. Three red-green-blue laser units, paired with laser speckle reducers, are coupled into endoscopic fiber optic light guides in a benchtop endoscope. Tissue phantom topography is reconstructed using alternating illumination of the laser units and a photometric stereo endoscopy algorithm. The contrast of flow regions is enhanced in an optical flow phantom using laser speckle contrast imaging. Further, the system retains the ability to offer white light and narrow band illumination modes with improved power efficiency, a reduced size, and longer lifetimes compared to conventional endoscopic arc lamp sources. This novel endoscopic light source design shows promise for increasing the detection of subtle lesions in routine colonoscopy screening.

Keywords

laser speckle reduction; photometric stereo; narrow band; laser speckle contrast imaging; endoscopy

1. INTRODUCTION

Colorectal cancer is the second most lethal variety of cancer with over 50,000 deaths expected to occur in the United States in 2019.[1] Widefield colonoscopy is considered the preventative standard of care for detecting and removing colorectal lesions prior to the onset of carcinoma. Studies on the efficacy of colonoscopy estimate that 1 in 5 colorectal lesions go undetected during routine colonoscopy, and nearly all of these lesions are under 10 mm in diameter with a sessile or flat appearance.[2, 3] In addition to being more difficult to detect, these non-polypoid lesions are more likely to be malignant in comparison to their polypoid counterparts.[4, 5] The risk of experiencing advanced stage or fatal interval cancer - the onset

Further author information: tbobrow1@jhmi.edu.

of cancer between routine screenings - strongly correlates with the adenoma detection rate of the physician providing treatment.[6] Thus, the incidence of colorectal mortality may significantly decline by improving adenoma detection rates, allowing for the removal of suspicious tissues prior to transforming into adenocarcinomas.

In recent years, endoscopic imaging capabilities have expanded to improve the contrast and detectability of lesions. For example, chromoendoscopy introduces topical dyes such as indigo carmine or methylene blue to the gastrointestinal lumen, strengthening the contrast of mucosal topography and tissue pathology.[7, 8] While shown to be highly effective, chromoendoscopy is rarely utilized for detection because of the resulting increase in screening procedure time.[9] Thus, focus has shifted to the investigation of optical enhancement methods such as narrow band imaging (NBI)[10] and autofluorescence imaging (AFI),[11] as well as image processing methods including Flexible Spectral Imaging Color Endoscopy (FICE)[12] and i-SCAN.[13]

We expand upon available image enhancement modalities through the introduction of a multimodal endoscope with adaptive-coherence, enabling switchable color, narrow band, texture, and flow imaging through a single endoscopic light source. We utilize red-green-blue (RGB) laser light for widefield endoscopic illumination, made possible by the use of laser speckle reduction to eliminate speckle artifacts that normally degrade image quality. In addition to a conventional white light imaging mode, narrow band illumination is implemented by toggling off the red diodes, and illuminating tissue with green-blue light for enhanced vasculature visualization. To enable topographic imaging, multiple RGB laser sources are sequentially toggled to illuminate imaged tissue from different angles, enabling reconstruction by photometric stereo. Flow imaging is made possible by temporarily switching off the laser speckle reducers, restoring speckle artifacts that are necessary for laser speckle contrast imaging. All of these modalities aim to enhance the contrast of key topographic and microcirculatory features that are highly indicative of dysplastic tissue.

2. METHODS

The endoscopic light source described in this work utilizes three RGB laser light sources (Aixiz, AIX-RGK-350) with 650nm-150mW, 532nm-80mW, and 450nm-120mW diodes combined on a single optical axis using dichroic mirrors. Each diode channel is equipped with a TTL trigger, allowing for individual diodes to be pulse width modulated and toggled on and off by a USB I/O controller (National Instruments, NI-9264). As shown in Figure 1, each laser module is condensed onto a laser speckle reducer, the output of which is collimated and refocused onto a 1.5 mm diameter endoscopic fiber bundle (Gulf Photonics, 12ft length, NA=0.55, fiber diameter=35um). The output face of the fiber bundle is coupled to an endoscopic light guide assembly (Advanced Power Group Corp., WTLGLA-187), equivalent to assemblies used in commercial endoscopes for diffusing output light onto imaged tissue.

Incident laser light produces a characteristic speckle appearance that adds noise and degrades the quality of captured images. These artifacts are produced by constructive and destructive interference between incident light waves as they independently scatter off

surfaces with wavelength-scale or greater roughness.[14] To mitigate speckle artifacts in our endoscopic image, we make use of laser speckle reducers (Optotune, LSR-3005-24D-VIS) constructed with electroactive polymer actuators that resonate a diffusion window at a frequency of 300 Hz.[15, 16]

Images were acquired using a dragonfly2 remote head camera with a 1/3 in color, 12 bit, 1032 776pixel CCD (Point Grey Research, Inc., DR2-08S2C-EX-CS). A board lens with a 145 deg field of view (M12 Lenses, PT-02120) was mounted to the detector to mimic the wide-angle view available in conventional endoscopes. A housing was 3d printed to mount the detector and the fiber optics 120 degrees apart from one another, at a 35 mm diameter concentric with the detector. A linear polarizing sheet (Thorlabs, LPVISE2X3) was laser cut and attached to the housing to polarize the light output of the fiber bundles. A linear polarizer (Edmund Optics, 47316) was mounted in front of the detector and adjusted to minimize specular reflection from the fiber output by cross-polarization. Frames were captured as RAW images and were demosaiced during post-processing.

2.1 White Light and Narrow Band Illumination

Conventional endoscopes utilize white light from a xenon arc lamp to illuminate tissue while performing endoscopic procedures. In recent years, a new narrow band imaging technique has been incorporated into commercial endoscopes by introducing a rotating filter wheel to the illumination source to increase the contrast of vasculature and tissue pathology.[17] Previous research in endoscopic illumination has used laser light for phosphor excitation to produce broadband white light as well as narrow band illumination by a single 410nm diode.[18] We choose to produce a narrow band illuminated image by toggling off the 650nm diode channels, illuminating tissue with 450nm and 532nm narrow band sources.

2.2 Photometric Stereo Endoscopy

Conventional endoscopes rely on multiple light sources positioned around the detector to eliminate shadow artifacts cast by tissue illuminated by a single point source. We opt to utilize information from single-source illumination to enhance the contrast of subtle topographic features by way of photometric stereo. Photometric stereo is a well-investigated computer vision technique in which sequential images are captured by a stationary detector while the scene is illuminated from multiple light source positions.[19] If one assumes a Lambertian remission model where observed light intensity varies as a function of surface normal to detector orientation, individual pixel intensities can be compared across sequential images to approximate surface normals. This task is accomplished by solving a simple system of linear equations,

$$\begin{bmatrix} S_{x1} & S_{y1} & S_{y1} \\ S_{x2} & S_{y2} & S_{y2} \\ S_{x3} & S_{y3} & S_{y3} \end{bmatrix} \begin{bmatrix} n_x \\ n_y \\ n_z \end{bmatrix} = \begin{bmatrix} m_1 \\ m_2 \\ m_3 \end{bmatrix} \quad (1)$$

where vector $s_i(x, y, z)$ represents the direction from surface to light source, vector $n(x, y, z)$ represents the surface normal, and m_i represents the measured intensity of a pixel in each of

the three frames. Light source location and pixel intensity are known, so surface normals can be estimated by solving for vector *n*. By integrating across surface normals using an inverse gradient multigrid solver,[20] tissue topography is estimated.

Photometric stereo requires the approximation of a perspective projection that is only valid when the field of view is narrow relative to the working distance of the camera. Endoscopic imaging presents a unique set of constraints for photometric reconstruction, as the large field of view and unknown working distance account for large errors in computation. To address these challenges, we utilize previous work in photometric stereo endoscopy (PSE)[21] that has increased lesion contrast in phantom models and *in-vivo*.[22] In this method, endoscopic imaging constraints are overcome by filtering out low frequency errors and retaining high-frequency information for reconstructing qualitative depth maps of the imaged colon

2.3 Laser Speckle Contrast Imaging

Laser speckle contrast imaging (LSCI) was first introduced as a method for enhancing the contrast of blood perfusion in the brain.[23] This modality relies on the imaging of scattered speckle artifacts that are used to distinguish static tissue and dynamic flow regions. The speckle pattern produced by a static turbid media remains constant if no sample, illumination source, or detector motion is introduced. On the contrary, superficial vasculature dynamically scatters coherent light with each new blood cell position. This cell and plasma motion results in a large number of speckle patterns produced over time, and results in a more homogeneous, speckle free region in the image when imaged with a relatively long integration time. By analyzing the deviation of speckle across an image, static tissue and vasculature flow regions can be differentiated and their contrast enhanced. Regions with a large number of distinguishable speckle interferences are indicative of a static tissue, while regions with a more homogeneous appearance are indicative of vasculature.

LSCI has been implemented both temporally by analyzing speckle deviation across several sequential frames, and spatially by examining individual frames for spatial deviation. We opt to implement a spatial, rolling window analysis method for efficient processing of speckle images.[24] In this method, a rolling average of standard deviation and mean are computed across an image using a window size of only a few pixels. A pixels speckle contrast value is computed using the window of surrounding pixels for which it is centered in,

$$k = \frac{\sigma_I}{\bar{I}} = \frac{\sqrt{\frac{\sum_{i=1}^{N}(I_i - \bar{I})^2}{N-1}}}{\bar{I}} \quad (2)$$

To demonstrate LSCI through a multimodal endoscope, we constructed phantom flow models using 1/64″ capillary tubing filled with 20% intralipid emulsion to represent a perfusing media. The intralipid was passed through the tubing using a programmable syringe pump (Braintree Scientific BS-9000-2). A silicone phantom doped with TiO_2 and India ink for scattering and absorption was placed below the capillary tubing to provide a similar effect as tissue beneath superficial vasculature in the colon.

3. RESULTS

We first evaluated the ability of the scope to reduce speckle artifacts in white light and narrow band illumination modes. By toggling the laser speckle reducers on, the cross-sectional motion of the diffusion window spatially varied the scattering of incident illumination through time. Over the detector integration time of several milliseconds or more, this allowed for the integration of several random scattering profiles to produce an image frame with reduced speckle, as shown in images of a Teflon target in Figure 2. By incorporating these laser speckle reducers into our light source, we minimized speckle artifacts that would otherwise contaminate an image captured by the scope.

We then evaluated the white light and narrow band illumination modes using *ex-vivo* porcine tissue. As shown in Figure 3, the scope successfully illuminated tissue samples using both white light and narrow band modes with no noticeable speckle artifacts. We also report the spectral contents of commercial white light and narrow band illumination modes in comparison to the output spectrum of multimodal light source used in this study. The laser narrow band sources closely align with commercially available narrow band wavelengths, but with thinner bandwidths.

Next, we reconstructed colon surface topography using photometric stereo. We utilized three laser illumination sources, synchronized with the detector frame rate of 15 Hz, to capture images from three equiangular illumination positions surrounding the detector. We applied this method to a silicone cecum phantom (Colonoscopy Trainer, The Chamberlain Group), and we used photometric stereo endoscopy to reconstruct high-frequency height maps of the imaged phantom following high-pass filtering of the images (kernel size and σ equal to 100 pixels). These image triads were then used to create high-frequency, photometric reconstructions. Figure 4 features reconstructions of a cecum phantom that makes subtle topographic features more visible and noticeable.

To assess the scopes ability to image flow regions, phantoms were imaged and processed using LSCI algorithms. In these experiments, images were captured using illumination from only the 532 nm diode channels with laser speckle reducers toggled off. Using this illumination, three different flow conditions were imaged: i.) capillary tubing containing only air ii.) capillary tubing containing intralipid with standing, Brownian motion iii.) intralipid actively pumped through the capillary tubing at a rate of 5 ml/min. LSCI images were then computed using a window size of 7x7 pixels. As displayed in Figure 5, the signal strength of the underlying capillary tubing increased when a liquid media was present to randomly scatter speckle through the cameras integration time. The capillary tubing with only air and no liquid media is not visible in the resulting laser speckle contrast image.

4. DISCUSSION

These results demonstrate that red-green-blue laser illumination, paired with laser speckle reducers, enables multiple illumination modes through one light source with the potential to increase the contrast of subtle lesion features. Adaptive switching of the laser speckle reducers effectively eliminated speckle in color, narrow band, and topographic modes that

would otherwise suffer from artifacts, while still providing sufficient speckle for LSCI while the speckle reducers were toggled off. Furthermore, photometric stereo reconstructions do not appear to suffer from any remaining speckle noise that is not eliminated by the speckle reducers. Laser speckle contrast images demonstrated sensitivity to flow regions, though no sensitivity to flow rate was observed. Sensitivity to flow rate may be improved by decreasing the detector integration time, limiting the number of captured random scattering events so that flow variation may be more easily distinguished.

It is not well understood how RGB laser illuminated images will differ from broadband illuminated images in endoscopy, as some pathologic features may require illumination outside of the laser narrow bandwidths in order to be effectively imaged. Future research should include comparison of tissue features in broadband and laser-illuminated images. To address color disparity amongst the three laser sources, more precise color balancing and fiber alignment would help eliminate color discrepancies seen in white light and narrow band illumination modes using laser light. Some inconsistencies may also be eliminated by randomizing the fiber bundle's individual fibers from input face to output face for effective color mixing. To achieve a narrow band image with the same qualities as commercialized NBI technology, image processing algorithms should be incorporated and applied to the narrow band illuminated images. Future expansion of this work may benefit from incorporating additional computer vision research. For example, deep learning has been applied to endoscopic imaging for both topographic reconstruction[25] and speckle reduction for laser illumination.[26]

5.CONCLUSION

In summary, we demonstrate an adaptive-coherence light source that is capable of photometric stereo for topographic reconstruction, laser speckle contrast imaging for vasculature contrast, narrow band imaging, and conventional color imaging. These imaging modalities show promise for increasing the detection and classification of colorectal lesions.

ACKNOWLEDGMENTS

This work was supported with funding from the NIH Trailblazer Award (R21EB024700).

REFERENCES

[1]. Siegel RL, Miller KD, and Jemal A, "Cancer statistics, 2019," CA: A Cancer Journal for Clinicians 69(1), 7–34 (2019). [PubMed: 30620402]

[2]. Lee J, Park SW, Kim YS, Lee KJ, Sung H, Song PH, Yoon WJ, and Moon JS, "Risk factors of missed colorectal lesions after colonoscopy," Medicine 96, e7468–e7468 (jul 2017). [PubMed: 28682916]

[3]. van Rijn JC, Reitsma JB, Stoker J, Bossuyt PM, van Deventer SJ, and Dekker E, "Polyp Miss Rate Determined by Tandem Colonoscopy: A Systematic Review," The American Journal of Gastroenterology 101, 343–350 (feb 2006). [PubMed: 16454841]

[4]. Soetikno RM, Kaltenbach T, Rouse RV, Park W, Maheshwari A, Sato T, Matsui S, and Friedland S, "Prevalence of Nonpolypoid (Flat and Depressed) Colorectal Neoplasms in Asymptomatic and Symptomatic Adults," JAMA 299, 1027–1035 (03 2008). [PubMed: 18319413]

[5]. Matsumoto Takayuki, Iida Mitsuo, T. Y. M. F., "Role of nonpolypoid neoplastic lesions in the pathogenesis of colorectal cancer," Diseases of the Colon & Rectum 37(5), 450–455 (1994). [PubMed: 8181406]

[6]. Corley DA, Jensen CD, Marks AR, Zhao WK, Lee JK, Doubeni CA, Zauber AG, de Boer J, Fireman BH, Schottinger JE, Quinn VP, Ghai NR, Levin TR, and Quesenberry CP, "Adenoma detection rate and risk of colorectal cancer and death," New England Journal of Medicine 370(14), 1298–1306 (2014).

[7]. Wallace MB and Kiesslich R, "Advances in endoscopic imaging of colorectal neoplasia," Gastroenterology 138(6), 2140 – 2150 (2010). Colon Cancer: An Update and Future Directions. [PubMed: 20420951]

[8]. Gáonzalez G, Parot V, Lo W, Vakoc BJ, and Durr NJ, [Feature Space Optimization for Virtual Chromoendoscopy Augmented by Topography], Springer International Publishing, Cham (2014).

[9]. Soetikno R, East J, Suzuki N, Uedo N, Matsumoto T, Watanabe K, Sanduleanu S, Sanchez-Yague A, and Kaltenbach T, "Endoscopic submucosal dissection for nonpolypoid colorectal dysplasia in patients with inflammatory bowel disease: in medias res," Gastrointestinal Endoscopy 87(4), 1085 – 1094 (2018). [PubMed: 29571773]

[10]. Machida H, Sano Y, Hamamoto Y, Muto M, Kozu T, Tajiri H, and Yoshida S, "Narrow-Band Imaging in the Diagnosis of Colorectal Mucosal Lesions: A Pilot Study," Endoscopy 36(12), 1094–1098 (2004). [PubMed: 15578301]

[11]. DaCosta RS, Wilson BC, and Marcon NE, [Optical Techniques for the Endoscopic Detection of Early Dysplastic Colonic Lesions], John Wiley & Sons, Ltd (2009).

[12]. Yoshida N, Naito Y, Inada Y, Kugai M, Inoue K, Uchiyama K, Handa O, Takagi T, Konishi H, Yagi N, Morimoto Y, Wakabayashi N, Yanagisawa A, and Yoshikawa T, "The detection of surface patterns by flexible spectral imaging color enhancement without magnification for diagnosis of colorectal polyps," International Journal of Colorectal Disease 27, 605–611 (May 2012). [PubMed: 22139031]

[13]. Hoffman A, Kagel C, Goetz M, Tresch A, Mudter J, Biesterfeld S, Galle P, Neurath M, and Kiesslich R, "Recognition and characterization of small colonic neoplasia with high-definition colonoscopy using i-scan is as precise as chromoendoscopy," Digestive and Liver Disease 42(1), 45 – 50 (2010). [PubMed: 19473893]

[14]. Goodman JW, "Some fundamental properties of speckle," J. Opt. Soc. Am. 66, 1145–1150 (Nov 1976).

[15]. Graetzel C, Suter M, and Aschwanden M, "Reducing laser speckle with electroactive polymer actuators," Proc.SPIE 9430, 9430 – 9430 – 8 (2015).

[16]. Farrokhi H, Rohith TM, Boonruangkan J, Han S, Kim H, Kim S-W, and Kim Y-J, "High-brightness laser imaging with tunable speckle reduction enabled by electroactive micro-optic diffusers," Scientific Reports 7(1), 15318 (2017). [PubMed: 29127389]

[17]. Kanao H, Tanaka S, Oka S, Hirata M, Yoshida S, and Chayama K, "Narrow-band imaging magnification predicts the histology and invasion depth of colorectal tumors," Gastrointestinal Endoscopy 69(3, Part 2), 631 – 636 (2009). Special issue: Colonoscopy for colorectal neoplasia. [PubMed: 19251003]

[18]. Togashi K, Nemoto D, Utano K, Isohata N, Kumamoto K, Endo S, and Lefor AK, "Blue laser imaging endoscopy system for the early detection and characterization of colorectal lesions: a guide for the endoscopist," Therapeutic advances in gastroenterology 9, 50–56 (jan 2016). [PubMed: 26770267]

[19]. Woodham RJ, "Photometric stereo: A reflectance map technique for determining surface orientation from image intensity," Proc.SPIE 0155, 0155 – 0155 – 8 (1979).

[20]. Farnebck G, Rydell J, Ebbers T, T. Andersson M, and Knutsson H, "Efficient computation of the inverse gradient on irregular domains," Proceedings of the IEEE International Conference on Computer Vision , 1–8 (01 2007).

[21]. Parot V, Lim D, González G, Traverso G, Nishioka NS, Vakoc BJ, and Durr NJ, "Photometric stereo endoscopy," Journal of biomedical optics 18, 76017 (jul 2013).

[22]. Durr N, J. Parot V, Traverso G, P. Puricelli W, Vakoc J, B. Nishioka N, and Gonzlez G, “Imaging colonic surface topography with photometric stereo endoscopy,” Gastrointestinal Endoscopy 79, AB459 (05 2014).

[23]. Boas DA and Dunn AK, “Laser speckle contrast imaging in biomedical optics,” Journal of biomedical optics 15(1), 11109 (2010).

[24]. Tom WJ, Ponticorvo A, and Dunn AK, “Efficient processing of laser speckle contrast images,” IEEE Transactions on Medical Imaging 27, 1728–1738 (Dec 2008). [PubMed: 19033089]

[25]. Mahmood F and Durr NJ, “Deep learning and conditional random fields-based depth estimation and topographical reconstruction from conventional endoscopy,” Medical Image Analysis 48, 230 – 243 (2018). [PubMed: 29990688]

[26]. Bobrow TL, Mahmood F, Inserni M, and Durr NJ, “DeepLSR: a deep learning approach for laser speckle reduction,” CoRR abs/1810.10039 (2018).

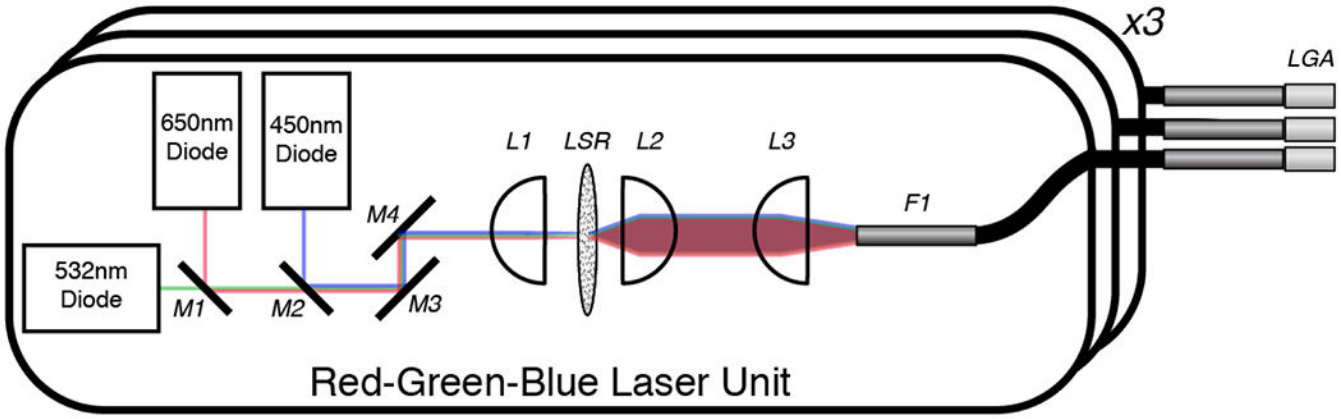

Figure 1.

Three fiber coupled RGB laser units are used to provide white light illumination for endoscopic imaging. 650mn, 532mn, and 450nm laser diodes are combined using dichroic mirrors (M1,M2). Reflective mirrors (M3,M4) are used to align the beam to an aspheric condenser lens (L1) which focuses the beam onto the clear aperture of a laser speckle reducer (LSR). Aspheric lenses (L2,L3) are used to collimate and refocus the light to the face of an endoscopic fiber bundle (F1). The output of the fiber bundle is coupled to an endoscopic light guide assembly (LGA) that diffuses the light, illuminating the scopes field of view.

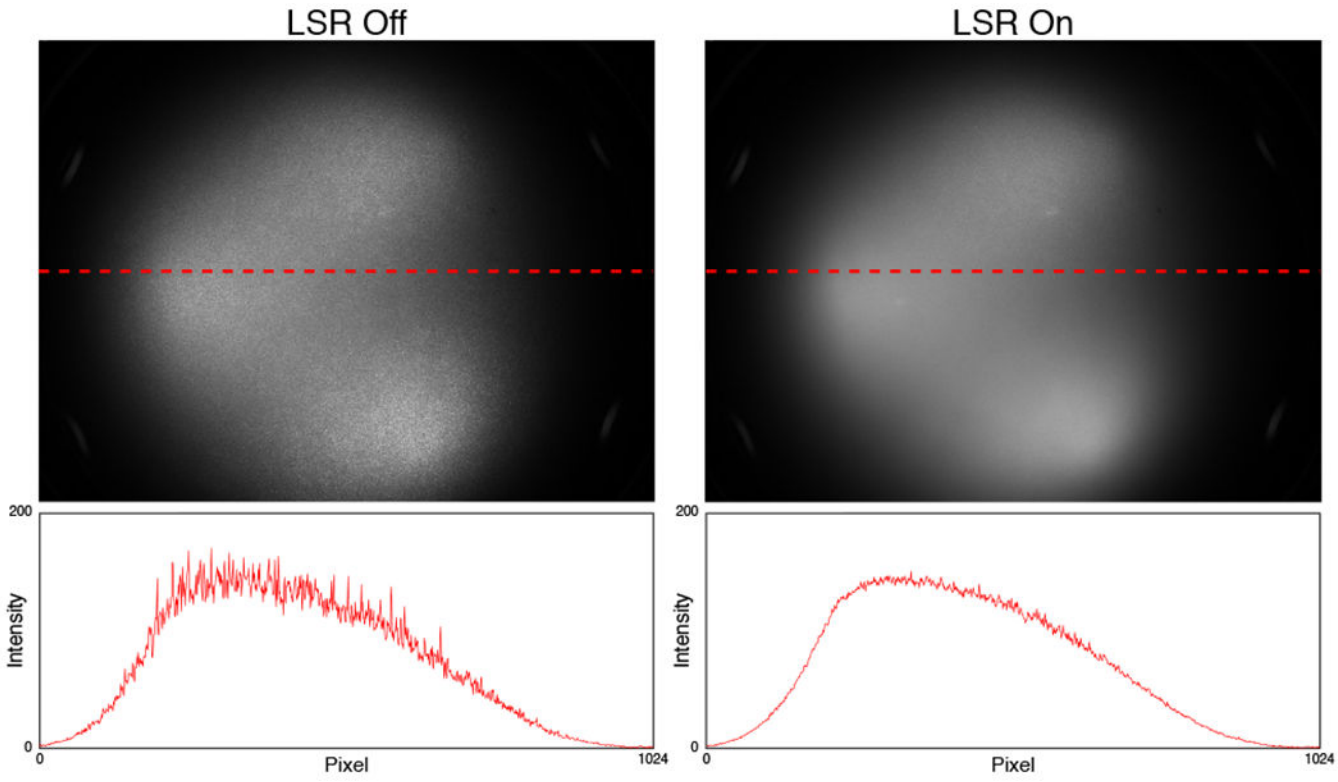

Figure 2.
Coherent light output imaged using a Teflon target. The LSR is toggled off (left) and on (right) to adaptively reduce speckle.

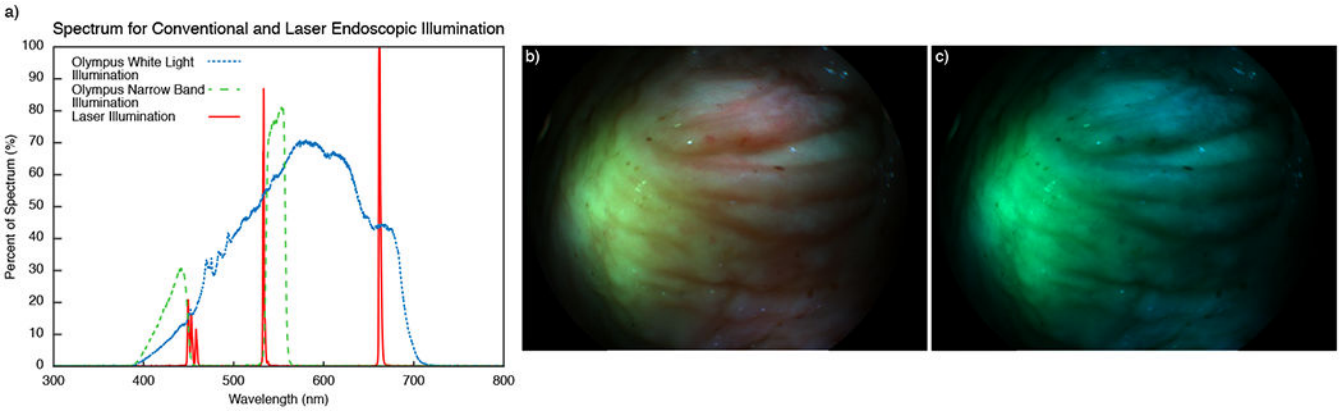

Figure 3.

(a) Spectral content of white light illumination and narrow band illumination modes available in a conventional endoscopic light source (Olympus, CLV-190) as well as the spectrum from the RGB lasers utilized in this study. Ex-vivo porcine colon was imaged using white light illumination from RGB laser light (b) as well as a narrow band mode using green-blue laser light (c), both with laser speckle reduction.

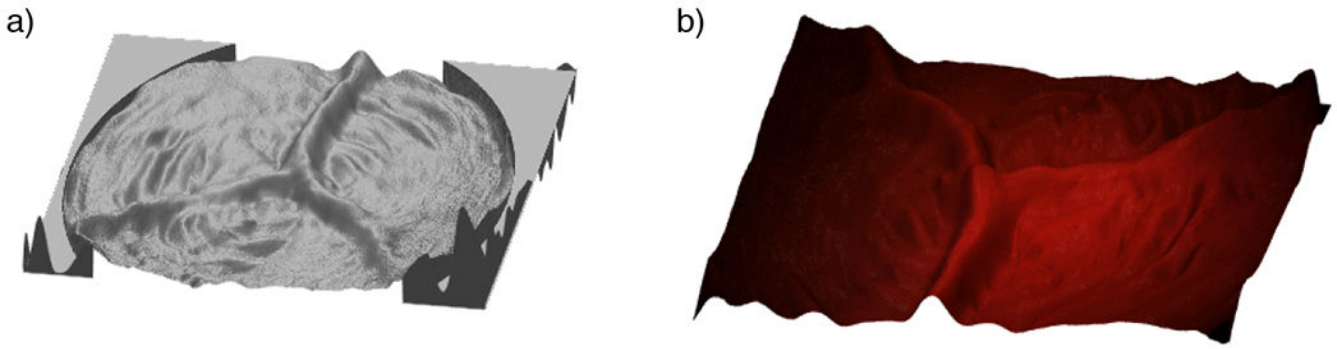

Figure 4.
Photometric stereo endoscopy using laser illumination. Images of a phantom captured with illumination from 60 deg, 180 deg, and 300 deg are used to create a topographic reconstruction (a). The three images are averaged to form a color image that is placed over the topography (b).

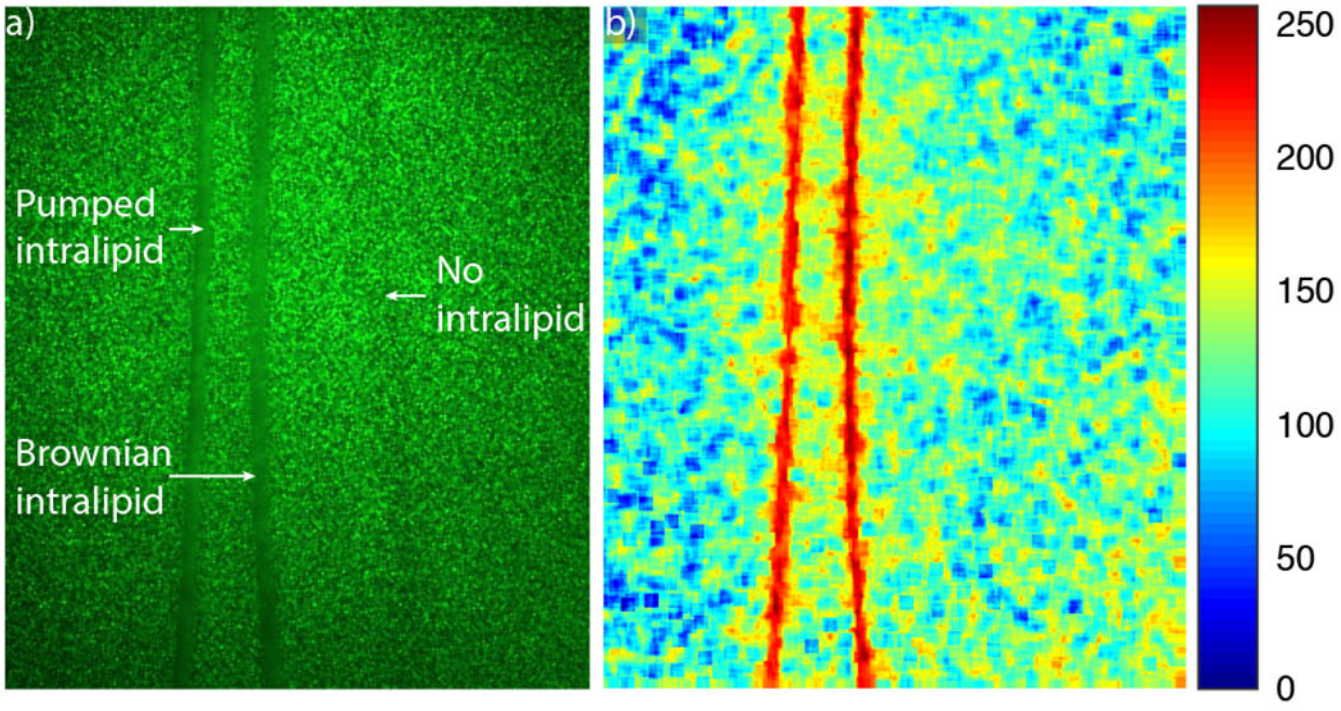

Figure 5.

Laser speckle contrast imaging. (a) An image of capillary tubing with no flow, intralipid with Brownian motion, and intralipid being actively pumped by a syringe pump. (b) the same image processed using LSCI spatial windowing algorithms. Signal strength increases with the presence of a liquid media.